

Efficient Estimation of Multiple Temperatures via a Collisional Model

Srijon Ghosh,^{1,*} Sagnik Chakraborty,^{1,†} and Rosario Lo Franco^{1,‡}

¹*Dipartimento di Ingegneria, Università degli Studi di Palermo, Viale delle Scienze, 90128 Palermo, Italy*

We present a quantum thermometric protocol for the estimation of multiple temperatures within the collisional model framework. Employing the formalism of multiparameter quantum metrology, we develop a systematic strategy to estimate the temperatures of several thermal reservoirs with minimal estimation error. We prove a necessary and sufficient condition for the singularity of the Fisher information matrix for a bi-parametrized qubit state. By using controlled rotations of ancillary systems between successive interaction stages, we eliminate parameter interdependencies, thereby rendering the quantum Fisher information matrix non-singular. Remarkably, we demonstrate that precision enhancement in the joint estimation of multiple temperatures can be achieved even in the absence of correlations among the ancillas, surpassing the corresponding thermal Fisher information limits. Exploiting correlations within the ancillary system yields additional enhancement of Fisher information. Finally, we identify the dimensionality of the ancillary systems as a key factor governing the efficiency of multiparameter temperature estimation.

I. INTRODUCTION

Estimating temperatures with precision has widespread applications ranging from assessing how hot the Earth is getting to measuring milli-Kelvin temperatures in a cold-atom Lab. Improving from the thick mercury thermometer lying around in every household, we have now ascended to using the energy levels of an atom to guess the temperature. In this regard, a very useful addition is quantum thermometry [1–13], where a small probe is sent out to interact and collect information about a bath, and then, using techniques of quantum estimation theory, the temperature of the bath is ascertained.

The problems of quantum thermometry can be formulated within the broader framework of parameter estimation theory [14–16], highlighting how temperature can be treated as an estimable quantity governed by the fundamental limits of quantum measurement. The primary prescription of the temperature estimation of a single bath is to thermalize a probe, having a specific heat C , to the environment with temperature T , and then measuring that probe provides the information about the temperature, which is fundamentally limited by $(\Delta T/T)^2 \geq k_B/C$. Over the last decade, various theoretical and experimental techniques have been proposed in the field of quantum thermometry. Apart from thermalizing the probe system, the collisional model [17, 18] has also been used to estimate the temperature of the environment, both in discrete and continuous variable models [19–21]. Starting from single quantum dots to NV centres in nanodiamonds have been designed as precise fluorescent thermometers [22–27]. Moreover, quantum harmonic oscillators [28], and Bose-Einstein condensate [29] have also been used to design quantum thermometers.

Interestingly, despite substantial recent progress in multiparameter quantum estimation theory [30–42], existing approaches have focused almost exclusively on the estimation of a single temperature. Perhaps surprisingly, the develop-

ment of protocols capable of estimating multiple temperatures remains largely unexplored. Here, we address this gap by developing a protocol for estimating multiple temperatures within a collisional model framework, leveraging tools from multiparameter phase estimation, where $\boldsymbol{\theta} = (\theta_1, \dots, \theta_N)^T$ is encoded in a quantum state $\rho(\boldsymbol{\theta})$. Suitable measurement reveals that the lower bound in measuring the uncertainty is given by the quantum Cramér Rao bound (QCRB), i.e., $\text{Cov}(\theta_1, \dots, \theta_N) \geq \mathcal{F}_Q^{-1}$, where $\text{Cov}(\theta_1, \dots, \theta_N)$ is the covariance matrix and \mathcal{F}_Q is the Quantum Fisher information matrix (QFIM).

In this paper, we develop a protocol based on a collisional model to estimate the temperatures of multiple thermal reservoirs maintained at different values. We begin by establishing a necessary and sufficient condition to avoid singularities in the estimation of minimum covariance between two temperatures encoded in an ancillary qubit. Building on this result, we introduce into our protocol a controlled unitary rotation which is applied between successive collisions of the qubit ancillas with the probes. We quantify the resulting enhancement of the Fisher information compared to standard temperature-estimation schemes. To assess the performance of the protocol, we define two figures of merit tailored to this multi-parameter estimation scenario. Our analysis reveals that even without preserving quantum correlations among the ancillas, our protocol offers a significant advantage compared to the thermal Fisher informations of the baths. Moreover, by exploiting the quantum correlations of the ancillas, the advantage can be further enhanced. Finally, we address the situation when the number of estimable temperatures is more than two, and in this scenario we discuss the necessity of higher-dimensional ancillas in our proposed framework.

The paper is organized as follows. We start by describing our protocol for estimating multiple temperatures using repeated probe-ancilla collisions in Sec. II. In Sec. III, we derive the necessary and sufficient condition for the singularity of the QFIM under certain conditions, and discuss the performance of the protocol for a single ancilla. Sec. IV deals with the effect of uncorrelated and correlated ancillas to acquire information about the thermal baths. The role and necessity of the higher-dimensional ancilla are discussed in Sec. V. We propose a possible experimental platform in Sec. VI. Finally, we

* srijon.ghosh@unipa.it

† sagnik.chakraborty@unipa.it

‡ rosario.lofranco@unipa.it

draw our conclusions in Sec . VII.

II. JOINT TEMPERATURE ESTIMATION PROTOCOL FOR MULTIPLE BATHS

Let us consider a collection of N non-interacting baths or thermal environments denoted by B_1, B_2, \dots, B_N with temperatures T_1, T_2, \dots, T_N , respectively. Let $\{S_1, \dots, S_N\}$ be N probe systems with local Hamiltonians $\{H_{S_1}, \dots, H_{S_N}\}$ each kept at thermal equilibrium with its corresponding bath. The thermalized probes carry information about their respective bath temperatures T_i 's ($i = 1, \dots, N$). To estimate these temperatures, we propose a collisional model framework where these probes are made to interact or “collide” according to a specific protocol with a stream of independent and identically prepared ancilla systems $\{A_k\}$ with $k = 1, 2, \dots, n$. Following this, appropriate measurements are performed on the ancillas, which reveal the information about the temperatures.

We consider a simple collision protocol between the ancillas and the baths. At first A_1 collides with S_1 . During this interaction A_1 acquired information about the first bath. A_1 is then rotated through a unitary $U_{rot}(\theta, \hat{r})$ for an angle θ around an axis \hat{r} . Simultaneously, the probe S_1 undergoes partial thermalization through a thermal map Λ_{S_1} for a time $t_{S_1 B_1}$ due to its coupling to the bath B_1 . This rotated A_1 then interacts with S_2 which is followed by another rotation $U_{rot}(\theta, \hat{r})$. This process of successive collision and rotation continues till the last collision with S_N , and then the ancilla is collected for measurement. This whole process is then repeated, starting with ancilla A_2 , followed by ancilla A_3 , and so on (see Fig. 1). At last, separate or joint measurements are performed on the ancillas to estimate the encoded parameters, i.e., temperatures of the multiple baths.

Initially, the system probes are thermalized with the respective baths, and the initial state of the i -th system is $\rho_{S_i}^{th}$. The initial state of the k -th ancilla is ρ_{A_k} . The system-ancilla interaction is governed by the unitary evolution $U_{S_i A_k}^i = \exp(-iH_{int}^{S_i A_k} t_{S_i A_k}^i)$ for a time interval $t_{S_i A_k}^i$ ($i = 1, \dots, N$). Here, $H_{int}^{S_i A_k}$ is the interaction Hamiltonian between the i -th system and k -th ancilla. The protocol follows three steps: first, the ancilla interacts with the first probe via $U_{S_1 A_k}^1$, and the resultant ancilla state reads as,

$$\begin{aligned} \tilde{\rho}_{A_k}(1) &= \mathcal{E}_{S_1 A_k}[\rho_{A_k}] \\ &= \text{Tr}_{S_1}[(U_{S_1 A_k}^1)(\Lambda_{S_1}^{k-1}[\rho_{S_1}^{th}] \otimes \rho_{A_k})(U_{S_1 A_k}^1)^\dagger] \end{aligned} \quad (1)$$

Here, $\Lambda_{S_1}^{k-1}[\rho_{S_1}^{th}]$ denotes the state of the first probe available to the k -th ancilla. Mathematically, Λ_{S_i} is defined as $\Lambda_{S_i}[\rho_{S_i}] = \gamma(\bar{n} + 1)\mathcal{K}[\sigma_{-}^{S_i}] + \gamma\bar{n}\mathcal{K}[\sigma_{+}^{S_i}]$ in the interaction picture, with $\mathcal{K}(O) = O\rho_{S_i}O^\dagger - 1/2\{OO^\dagger, \rho_{S_i}\}$ and $\sigma_{\pm}^{S_i}$ being the raising and lowering operators acting on the probe S_i . γ is the time-independent coupling constant, and \bar{n} is the thermal occupation number. This is followed by the rotation of the ancillary system, given by

$$\tilde{\rho}_{A_k}(1) = \mathcal{U}_{rot}[\tilde{\rho}_{A_k}(1)] = U_{rot}(\theta, \hat{r}) \tilde{\rho}_{A_k}(1) U_{rot}(\theta, \hat{r})^\dagger.$$

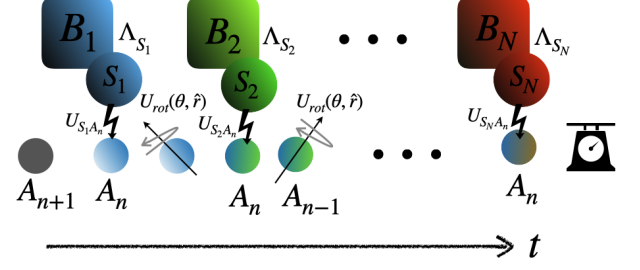


FIG. 1. Schematic representation of the multiparameter temperature estimation protocol based on the collisional model. The information about the first bath, B_1 , is acquired by the n -th ancilla through its interaction with the probe system S_1 . A controlled unitary rotation is subsequently applied to the ancilla A_n , after which it interacts with the next probe to extract information about the second bath, B_2 . This sequence is iteratively repeated for all N thermal reservoirs.

At last, the resultant ancilla interacts with the next bath S_2 , and the process continues. The resultant ancilla after N successive collisions and rotations looks like

$$\rho_{A_k}^f(N) = \mathcal{U}_{rot} \circ \mathcal{E}_{S_N A_k} \circ \dots \circ \mathcal{U}_{rot} \circ \mathcal{E}_{S_1 A_k} [\rho_{A_k}]. \quad (2)$$

Here, $\rho_{A_k}^f(N)$ denotes the final state of the k -th ancilla. The protocol now continues for n ancillas, and the final joint state of the ancillas, $\rho_{A_1 \dots A_n}$, is measured via a positive operator valued measurement (POVM) $\{\Pi_j\}_j$ (j is the possible outcome), which provides the Fisher information matrix $F(N)$. Maximizing over all such POVMs provides the QFIM $\mathcal{F}_Q^{(N)}$, whose (i, j) element is defined by, $(\mathcal{F}_Q)_{ij} = \frac{1}{2}\text{Tr}[\rho_{A_1 \dots A_n}^f(L_i L_j + L_j L_i)]$. Note that L_μ is the symmetric logarithmic derivative (SLD) corresponding to the temperature T_μ given by $\frac{\partial \rho_{A_1 \dots A_n}^f}{\partial T_\mu} = \frac{1}{2}[L_\mu \rho_{A_1 \dots A_n}^f + \rho_{A_1 \dots A_n}^f L_\mu]$.

Performance indicator: Here we consider two figures of merit to compare our protocol with the scenario when the temperature of the individual baths is estimated separately using their respective thermal Fisher informations \mathcal{F}_{th}^i . We compare the efficiency of our protocol by constructing a $N \times N$ thermal Fisher information matrix \mathcal{F}_{th} for N baths.

Suppose a probe is in thermal contact with a bath having inverse temperature $\beta = 1/k_B T$, where k_B is the Boltzmann constant. The completely thermalized state of the system is $\rho_{S_i}^{th} = \exp(-\beta H_{S_i})/\exp(-\beta H_{S_i})$, where H_{S_i} is the local Hamiltonian of the probe. Then, the thermal Fisher information acquired from the system is given by

$$F_{th}^i = \frac{\langle H_{S_i}^2 \rangle - \langle H_{S_i} \rangle^2}{k_B^2 T^4}. \quad (3)$$

where $\langle \bullet \rangle$ denotes the average value of an operator. Using this, we construct the thermal Fisher information matrix \mathcal{F}_{th} as $\mathcal{F}_{th} = \text{diag}(F_{th}^1, F_{th}^2, \dots, F_{th}^N)$. F_{th}^i is the thermal Fisher information for the i -th probe. In this scenario, the total input

state is $\rho_{th} = \otimes_{i=1}^N \rho_{S_i}^{th}$ and $\rho_{S_i}^{th}$ only contains the information about the i -th bath. Note that the construction of \mathcal{F}_{th} has been designed to serve as a benchmark for our proposed protocol. We compare these two Fisher information matrices \mathcal{F}_Q and \mathcal{F}_{th} and *total average information* as,

$$\eta_{\text{joint}} = \frac{\text{Tr}(\mathcal{F}_Q)}{\text{Tr}(\mathcal{F}_{th})}. \quad (4)$$

Here, $\eta_{\text{joint}} < 1 (> 1)$ indicates that the joint information contained in \mathcal{F}_Q is smaller (larger) than \mathcal{F}_{th} . Note that η_{joint} does not consider the effect of the correlation between different parameters. However, we also define another performance indicator, *information accuracy*,

$$\eta_{\text{acc}} = \log \left[\frac{\det(\mathcal{F}_Q)}{\det(\mathcal{F}_{th})} \right], \quad (5)$$

that captures the effect of correlation among the parameters, and also ensures the minimum error condition. The positive value of η_{acc} indicates that the lower bound of error in the joint estimation protocol is less than \mathcal{F}_{th} . On the other hand, a negative value implies that the estimation protocol has a large lower bound in the error estimation. In the rest of the manuscript, we will use these two indicators to compare the effectiveness of our proposed protocol.

III. SINGLE-RUN TEMPERATURE ESTIMATION

We begin by considering the simplest model, consisting of two probes, each of which is fully thermalized with its respective bath. A single ancilla interacts with these probes sequentially to acquire information about the bath parameters. In multiparameter estimation, one of the central difficulties arises from the singularity of the QFIM (\mathcal{F}_Q), i.e., \mathcal{F}_Q^{-1} does not exist. This leads to an unbounded lower bound on the estimation uncertainty. This divergence reflects an intrinsic inefficiency in the design of the protocol. Such singularities can occur for various reasons [43], one of which is that the parameters of interest may become functionally dependent. Consequently, an efficient multiparameter estimation scheme must explicitly account for this issue. In our proposed protocol, a controlled unitary rotation introduced between the two encoding stages eliminates these parameter dependencies. In this regard, we now proceed to prove the following theorem:

Theorem 1. For any bi-parameterized qubit state, $\eta(\xi_1, \xi_2)$ the QFIM $\mathcal{F}_Q(\eta)$ is non-invertible, i.e., $\det(\mathcal{F}_Q(\eta)) = 0$ if and only if

$$\frac{\partial \eta}{\partial \xi_1} = c \frac{\partial \eta}{\partial \xi_2} \quad (6)$$

for some real number c .

Proof. It can be easily seen that the theorem holds true for the trivial case $\frac{\partial \eta}{\partial \xi_1} = 0$ or $\frac{\partial \eta}{\partial \xi_2} = 0$ by choosing $c = 0$. We therefore consider the non-trivial scenario where neither of the derivatives is zero. It ensures that the SLD operators L_i 's

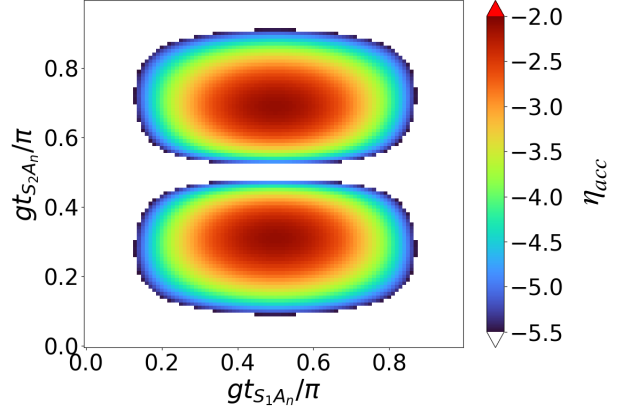


FIG. 2. The variation of η_{acc} is illustrated for the case where a single ancilla sequentially interacts with the first and second probes, with interaction strengths $gt_{S_1 A_n}/\pi$ and $gt_{S_2 A_n}/\pi$, respectively. Here, $K_B T_{B_1}/\hbar\omega = 2$, and $K_B T_{B_2}/\hbar\omega = 1$.

are non-zero and \mathcal{F}_Q is either rank 1 or 2. Using the spectral decomposition $\eta = \alpha_0 |\alpha_0\rangle\langle\alpha_0| + \alpha_1 |\alpha_1\rangle\langle\alpha_1|$ the QFIM can be written as

$$\mathcal{F}_Q(\eta) = \frac{1}{2} \alpha_0 (M_0 + M_0^*) + \frac{1}{2} \alpha_1 (M_1 + M_1^*) \quad (7)$$

where M^* denotes complex conjugate of a matrix M , and, M_0 and M_1 are positive matrices given by $M_0 = W_0 W_0^\dagger$ and $M_1 = W_1 W_1^\dagger$, where

$$W_0 = \begin{pmatrix} \langle\alpha_0|L_1 \\ \langle\alpha_0|L_2 \end{pmatrix} ; \quad W_1 = \begin{pmatrix} \langle\alpha_1|L_1 \\ \langle\alpha_1|L_2 \end{pmatrix} \quad (8)$$

Note that the SLD operators can be expressed as

$$L_i = \sum_{j,k=0,1} \frac{2 \langle\alpha_j| \frac{\partial \eta}{\partial T_i} |\alpha_k\rangle}{\alpha_j + \alpha_k} |\alpha_j\rangle\langle\alpha_k| \quad (9)$$

Also note that the rank of any M^* is always equal to that of M . It can be easily seen from Eq. (9) that condition (6) is equivalent to

$$\langle\alpha_0|L_1|\alpha_0\rangle = c \langle\alpha_0|L_2|\alpha_0\rangle \quad (10)$$

$$\langle\alpha_0|L_1|\alpha_1\rangle = c \langle\alpha_0|L_2|\alpha_1\rangle \quad (11)$$

$$\langle\alpha_1|L_1|\alpha_1\rangle = c \langle\alpha_1|L_2|\alpha_1\rangle \quad (12)$$

Therefore, if condition (6) is true then from Eqs. (10), (11) and (12) we can conclude that $\langle\alpha_0|L_1 = c \langle\alpha_0|L_2$ and $\langle\alpha_1|L_1 = c \langle\alpha_1|L_2$. This implies

$$W_0 = \begin{pmatrix} c \langle\alpha_0|L_2 \\ \langle\alpha_0|L_2 \end{pmatrix} ; \quad W_1 = \begin{pmatrix} c \langle\alpha_1|L_2 \\ \langle\alpha_1|L_2 \end{pmatrix} \quad (13)$$

As a result, we get

$$\mathcal{F}_Q(\eta) = (\alpha_0 \langle\alpha_0|L_2^2|\alpha_0\rangle + \alpha_1 \langle\alpha_1|L_2^2|\alpha_1\rangle) \begin{bmatrix} c \\ 1 \end{bmatrix} \begin{bmatrix} c & 1 \end{bmatrix}$$

which clearly implies $\mathcal{F}_Q(\eta)$ is rank 1 and as a result $\det(\mathcal{F}_Q(\eta)) = 0$. This proves the first part of the theorem.

We now show if condition (6) is violated, \mathcal{F}_Q is rank 2 and consequently $\det(\mathcal{F}_Q(\eta)) \neq 0$. From the equivalence of condition (6) and Eqns. (10), (11) and (12) we can conclude that if condition (6) is violated at least one of the following inequalities are true

$$\frac{\langle \alpha_0 | L_1 | \alpha_0 \rangle}{\langle \alpha_0 | L_2 | \alpha_0 \rangle} \neq \frac{\langle \alpha_0 | L_1 | \alpha_1 \rangle}{\langle \alpha_0 | L_2 | \alpha_1 \rangle} \quad (14)$$

$$\frac{\langle \alpha_1 | L_1 | \alpha_0 \rangle}{\langle \alpha_1 | L_2 | \alpha_0 \rangle} \neq \frac{\langle \alpha_1 | L_1 | \alpha_1 \rangle}{\langle \alpha_1 | L_2 | \alpha_1 \rangle} \quad (15)$$

Inequality (14) implies W_0 is rank 2, and, inequality (15) implies W_1 is rank 2. Thus at least one of W_0 or W_1 is rank 2, which in turn means \mathcal{F}_Q is rank 2. \square

Suppose the local Hamiltonian of the two baths and the ancilla are $H_{S_i} = \omega_{S_i} \sigma_z/2$ ($i = 1, 2$) and, $H_{A_1} = \omega_{A_1} \sigma_z/2$ respectively. The interaction Hamiltonian between the system and ancilla is given by, $H_{S_i A_1} = g_i(\sigma_+ \otimes \sigma_- + \sigma_- \otimes \sigma_+)$. Let us consider the initial state of the ancilla to be ρ_{A_1} , and the thermalized probe is in a state $\rho_{S_i}^{th} = \sum_k \lambda_k(T_i) |k\rangle \langle k|$ which are thermalized with the corresponding bath having temperature T_i . The action of the collision is given by

$$\mathcal{E}_{T_1}[\rho_{A_1}] = Tr_{S_1} [U_{S_1 A_1}(\rho_{S_1}^{th}(T_1) \otimes \rho_{A_1}) U_{S_1 A_1}^\dagger]$$

Now for two consecutive collisions of the ancilla with the first and the second bath, we have $\hat{\mathcal{E}}_f = \hat{\mathcal{E}}_{T_2} \cdot \hat{\mathcal{E}}_{T_1}$. Note that $\hat{\bullet}$ indicates the vectorized form of the operators. For the sake of simplicity, we take the interaction strengths to be identical, i.e., $g_1 = g_2$ and $t_{S_1 A_1} = t_{S_2 A_1} = t$. Now, if the initial ancilla state is $\rho_{A_1} = |1\rangle \langle 1|$, we get $\mathcal{E}_f[\rho_{A_1}] = \hat{\Lambda}_f \cdot \rho_{A_1} \hat{\Lambda}_f$ (for detailed calculation, see Appendix. A), i.e.,

$$\rho_{A_1}^f = \mathcal{E}_f[\rho_{A_1}] = \begin{bmatrix} v(T_1, T_2) & 0 \\ 0 & 1 - v(T_1, T_2) \end{bmatrix}, \quad (16)$$

where $v(T_1, T_2) = \sin^2 gt [p + q \cos^2 gt]$ with $p = \lambda_0(T_1)$ for $\hat{\mathcal{E}}_{T_1}$ and $q = \lambda_0(T_2)$ for $\hat{\mathcal{E}}_{T_2}$.

It can be easily seen that $\frac{\partial \rho_{A_1}^f}{\partial T_1} = [(\frac{\partial v}{\partial T_1}) / (\frac{\partial v}{\partial T_2})] \frac{\partial \rho_{A_1}^f}{\partial T_2}$. Thus, using Theorem 1, we must have $\det(\mathcal{F}_Q(\rho_{A_1}^f)) = 0$. Moreover, the exact form of the QFIM in this case is given by

$$\mathcal{F}_Q(\rho_{A_1}^f) = \frac{1}{v(1-v)} \begin{bmatrix} (\partial_1 v)^2 & (\partial_1 v)(\partial_2 v) \\ (\partial_2 v)(\partial_1 v) & (\partial_2 v)^2 \end{bmatrix} \quad (17)$$

As can be easily seen here, $\det(\mathcal{F}_Q) = 0$, which implies that the protocol automatically makes the two parameters dependent. In order to avoid this issue, we introduce a rotation $U_{rot}(\pi/4, \hat{x}) = \exp(-i\pi\sigma_x/4)$ between two successive collisions as shown in Fig. 1. Thus, $\hat{\mathcal{E}}_f$ is given by

$$\hat{\mathcal{E}}_f = \hat{\mathcal{E}}_{T_2} \cdot \hat{\mathcal{U}}_{rot} \cdot \hat{\mathcal{E}}_{T_1} \quad (18)$$

One can easily see that $\rho_{A_1}^f = \mathcal{E}_f[\rho_{A_1}] = \hat{\mathcal{E}}_f \cdot \rho_{A_1}^f$ is in the form

$$\rho_{A_1}^f = \begin{bmatrix} \mu(q) & -i\chi(p) \\ i\chi(p) & 1 - \mu(q) \end{bmatrix} \quad (19)$$

where $\mu(q) = \frac{1}{4}[(1+2q)+(1-2q)\cos 2g]$ and $\chi(p) = \frac{1}{2}[(1-p)+p\cos 2g]$. Now, $\frac{\partial}{\partial T_1}(\rho_{A_1}^f) = \dot{\chi}\sigma_y$ and $\frac{\partial}{\partial T_2}(\rho_{A_1}^f) = \dot{\mu}\sigma_z$, where $\dot{\mu} = d\mu/dT_2$ and $\dot{\chi} = d\chi/dT_1$. Using Theorem 1 we can conclude $\det(\mathcal{F}_Q) \neq 0$.

Since in this case $[L_1, L_2] \neq 0$ (see Appendix A), the two temperatures cannot, in general, be estimated simultaneously. Nevertheless, within the framework of our protocol, one can appropriately tune the free parameters and reach an estimation strategy that is closest to the simultaneous measurement scenario. In particular, the achievable Fisher information for both baths can be made comparable to their respective thermal Fisher information. For a single-collision protocol, one typically expects the information-accuracy η_{acc} to be negative, indicating that the lower bound on temperature estimation in our scheme is higher than the bound set by $\mathcal{F}_{th} = \text{diag}(0.015, 0.197)$ (from Eq. 3). However, as shown in Fig. 2, there exist certain collision strengths even within a single-run scenario for which η_{acc} gets closer to zero, although still being negative. We observe that when $gt_{S_1 A_1}/\pi = 0.5$, the protocol attains the maximum value of η_{acc} , or in other words, the minimum estimation uncertainty predicted by the QCRB. Note that this value makes the interaction unitary between the ancilla and the first bath to be a SWAP operation with an imaginary phase. On the other hand, the total information jointly accessible about the two parameters does not depend on the specific nature of the first collision. However, to achieve the maximum value of η_{joint} , the second interaction must effectively implement a phased-SWAP operation. Typically, to obtain the maximum joint information about the parameters, one should fix the interaction strength so that a phased-SWAP operation is performed on both probes. However, the estimation uncertainty becomes considerably larger at this interaction strength, indicating a clear trade-off between η_{joint} and η_{acc} . Taking this into account, we exclude this regime from our analysis. In the remainder of the manuscript, we fix the interaction strength between the ancilla and the first bath such that this phased-SWAP operation is reproduced.

IV. INFORMATION ACQUIRED THROUGH MULTIPLE COLLISIONS

Previous analysis based on a single-collision setup shows that, for specific values of the interaction strength, it becomes possible to extract information about the parameters of interest within well-defined error bounds. Let us now discuss whether it is possible to gain more information by exploiting multiple ancillary systems. Here we consider two specific scenarios: one, performing a joint measurement on the resultant product ancilla state of the n qubits (where n is the total number of ancilla) following the protocols as described in Sec. II.

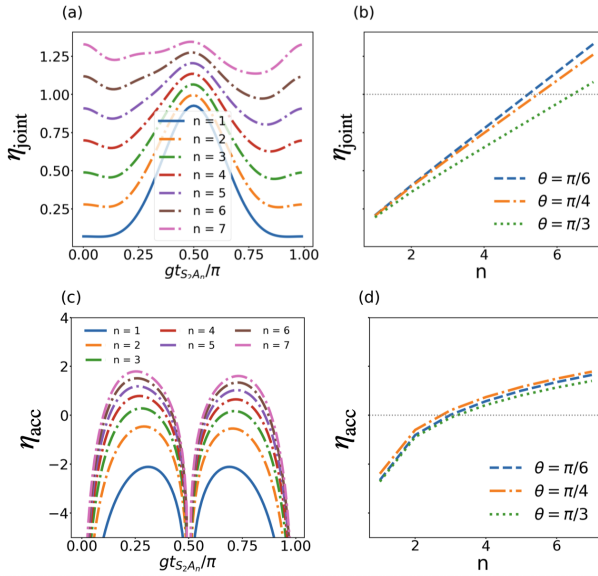


FIG. 3. The trend of η_{joint} and η_{acc} with respect to coupling strength for different numbers of uncorrelated ancillas n ((a) and (c)). Here $gts_{1A_n}/\pi = 0.5$ and $\gamma t_{S_iB_i} = 0.5$ for $i = 1, 2$. (b) and (d) denotes the scaling of η_{joint} , and η_{acc} for different angles of rotation around the x -axis. The dotted horizontal lines in (b) and (d) indicate $\eta_{\text{joint}} = 1$ and $\eta_{\text{acc}} = 0$ respectively i.e., $\mathcal{F}_Q = \mathcal{F}_{th}$. All other details are the same as Fig. 2.

Secondly, we analyze the situation when the ancillary systems get correlated due to the successive interaction with the same probe systems.

Effect of uncorrelated multiple ancilla: A systematic analysis reveals that employing multiple ancillary systems provides a significant advantage within the proposed protocol. Even in the absence of correlations among the ancillas, performing a global measurement on their joint state enables the extraction of more information than in the single-collision scenario. As illustrated in Fig. 3(a), when the number of ancillas exceeds three, the performance of our protocol surpasses the joint information contained in \mathcal{F}_{th} , i.e., $\eta_{\text{joint}} > 1$. In this regime, a finite error bound is also achievable, as shown in Fig. 3(c). Intuitively, after each interaction with an ancilla, the individual probe systems are allowed to partially thermalize with their respective baths. As a result, when the next ancilla interacts with the probe, the probe has already acquired additional information from its corresponding bath. This repeated interaction of the probe with the bath between successive ancilla collisions provides an advantage over the single-collision model, even in the absence of any correlations between the ancillas.

Moreover, after more than three collisions, the maximum numerical value of η_{acc} becomes positive, indicating that the estimation error in our protocol is lower than the corresponding thermal Fisher-information bound. The scaling of η_{joint} with respect to the number of ancillas, presented in Fig. 3(b), demonstrates that it increases monotonically; hence, larger numbers of ancillas yield progressively more joint information about the bath temperatures. Nevertheless, Fig. 3(d) suggests that the error eventually saturates as the number of col-

lisions grows. Despite this saturation, the error bound remains considerably tighter than in the thermal scenario, since $\eta_{\text{acc}} > 0$ even after three consecutive collisions.

It is also worth noting that each ancilla undergoes the same rotation by an angle θ . While $\theta = \pi/6$ yields slightly higher joint information, the error bound is minimized for $\theta = \pi/4$, where η_{acc} reaches its maximum. Consequently, in our subsequent analysis of the influence of correlations between ancillas, we focus exclusively on the case $\theta = \pi/4$.

Information gain from ancilla correlation: Up to this point, we have examined the scenario in which the ancillas, despite undergoing repeated interactions with the same probe system, remain uncorrelated under our proposed protocol. We now turn to the case where the ancillas are correlated, in which the final state of the ancillary systems, from which the information about the two baths ($N = 2$) must be extracted, is given by

$$\rho_{A_1 \dots A_n} = \text{Tr}_{S_1 S_2} \left[\Lambda_{S_2} \circ \mathcal{U}_{\text{rot}}^{A_n} \circ \mathcal{U}_{S_2 A_n} \circ \dots \circ \Lambda_{S_2} \circ \mathcal{U}_{\text{rot}}^{A_2} \circ \mathcal{U}_{S_2 A_1} \circ \Lambda_{S_1} \circ \mathcal{U}_{\text{rot}}^{A_1} \circ \mathcal{U}_{S_1 A_1} (\rho_{th}^{S_1} \otimes \rho_{th}^{S_2} \otimes \rho_{A_{k+1}}^{\otimes n}) \right]. \quad (20)$$

Here $\mathcal{U}_{\text{rot}}^{A_i}$ denotes the rotation is applied in the A_i -th ancilla. Performing suitable measurements on the joint ancilla state $\rho_{A_1 \dots A_n}$ reveals that for $n = 2$, the correlated and uncorrelated scenarios provide almost identical values of the joint information and accuracy bound (see Fig. 4). However, when the number of ancillary systems is increased, the correlations established among them provide a significant advantage over both the uncorrelated case and, naturally, the thermal reference scenario. Moreover,

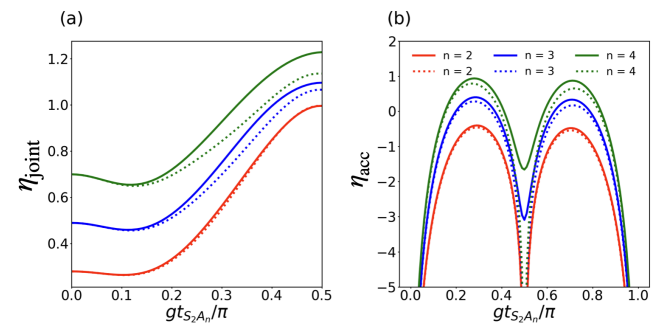


FIG. 4. Comparison between correlated (solid lines) and uncorrelated ancilla (dotted lines) for (a) η_{joint} and (b) η_{acc} with respect to the interaction strength. Here, $gts_{1A_n} = 0.5$. All other details are similar to Fig. 3.

η_{acc} increases substantially, demonstrating that our proposed protocol is highly efficient in accurately inferring the temperatures of the two baths.

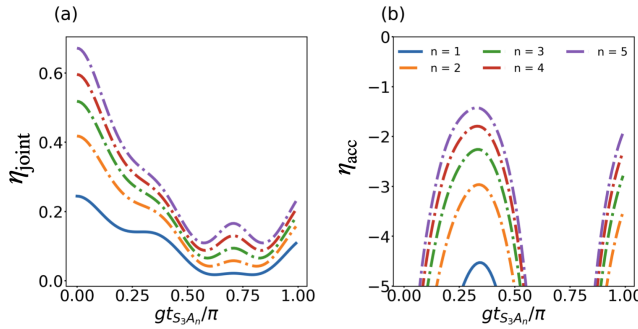


FIG. 5. The behaviour of (a) η_{joint} and (b) η_{acc} with respect to the interaction strength of the qutrit with the last probe. Here, $gts_{1A_n} = 0.5$, $gts_{2A_n} = 0.2$ and $K_B T_{B3}/\hbar\omega = 3$. All other details are similar to Fig. 3.

V. ROLE OF HIGHER-DIMENSIONAL ANCILLA IN THE ESTIMATION PROTOCOL

In this section, we examine the problem of temperature estimation involving three thermal baths, corresponding to $N = 3$. We begin by considering two-dimensional ancillary systems employed to encode information about the baths. Since a qubit possesses three degrees of freedom, it is, in principle, capable of encoding three independent parameters [36]. Nevertheless, it has been shown that under unitary encoding, the simultaneous estimation of multiple parameters becomes infeasible when the number of parameters exceeds the dimension of the probe, as the Fisher information matrix turns singular. Consequently, no finite bound on the estimation precision can be established [38]. In our proposed protocol, although the encoding process is modelled as a general completely positive trace-preserving (CPTP) map rather than a strictly unitary evolution, we observe a similar limitation. While the qubit can, in principle, carry information about three distinct temperatures, the parameter η_{acc} becomes significantly negative, indicating that the achievable error bound within this scheme is highly unsatisfactory.

To avoid this hurdle, we consider a collisional model consisting of identically prepared qutrit systems to encode and decode the information of the baths. To make the analysis coherent, we consider an energy-conserving interaction Hamiltonian between the i -th qubit probe and the n -th qutrit ancilla with the identical interaction strength, given by, $H_{S_i A_n} = g(\sigma_+ \mathcal{Q}_- + \sigma_- \mathcal{Q}_+)$. Here, $\mathcal{Q}_\pm = (S_x \pm iS_y)/2$ with S_ν ($\nu = x, y$, and z) denote the higher-dimensional Pauli operators and g is the interaction strength.

Fig. 5(a) indicates that achieving sufficient information about the system—while maintaining a decent lower bound on the estimation error—requires the coupling strength between the third bath and each ancilla to be approximately comparable to the interaction strength with the second probe. Increasing the dimension of the ancillary systems further ensures a finite lower bound on the estimation error, as illustrated in Fig. 5(b). Additionally, enlarging the number of an-

cillas enhances the achievable precision, consistent with the behavior observed in the uncorrelated two-bath scenario. Although the case $n = 5$ does not surpass the thermal precision limit given by $\mathcal{F}_{\text{th}} = \text{diag}(0.015, 0.197, 0.003)$, it is evident that sufficiently many ancillas will do so. As before, each ancilla undergoes a unitary rotation between successive interactions with the probe systems. These observations collectively demonstrate that our protocol enables accurate joint temperature estimation of N baths, provided that the ancilla dimension is chosen appropriately.

VI. PROPOSED EXPERIMENTAL FRAMEWORK

The theoretical architecture considered here—namely, a sequence of two-level systems interacting one at a time with single-mode cavities that, between interactions, relax toward a thermal state—is the standard framework of micromaser and Rydberg cavity-QED physics. In these systems, the intracavity field dissipates into a thermal reservoir, and changes in accordance with a damped harmonic-oscillator master equation while the individual Rydberg atoms traverse a high-Q superconducting cavity undergoing coherent Jaynes–Cummings interactions. In cavity QED with Rydberg atoms, this description is well established at the phenomenological and microscopic levels [44, 45]. Moreover, between the cavities, a suitably chosen laser field rotates the Rydberg atom in the desired direction [46], thereby implementing the unitary rotation required by our protocol.

A solid-state implementation of the same physics is provided by circuit quantum electrodynamics, or circuit QED. The Jaynes–Cummings (or quantum Rabi) Hamiltonian of atomic cavity QED governs the interaction between planar or three-dimensional microwave resonators, which offer single electromagnetic modes, and superconducting qubits, which operate as artificial two-level atoms. Since Blais et al.’s seminal proposal, in which the circuit-QED model replicates the canonical atom–cavity interaction with similar rotating-wave couplings and open-system channels driving cavity decay into electromagnetic baths [47], this equivalence has been made clear. According to recent studies, circuit QED is an on-chip version of atomic cavity QED with the same light-matter Hamiltonians, controllable dissipation, and designed surroundings [48, 49].

These findings demonstrate that, while retaining the same Hamiltonian structure, dissipative mechanisms, and sequential interaction paradigm as in atomic cavity QED, the cascaded cavity-QED model studied here can be replicated in a superconducting platform with artificial atoms and planar microwave cavities.

VII. CONCLUSIONS

In this work, we have developed a multitemperature estimation protocol based on a collisional model and analyzed its fundamental limitations and achievable precision. We identified a necessary and sufficient condition for the singularity of

the Fisher information matrix (FIM) when thermal information about two baths is encoded in a single qubit probe. By incorporating a controlled unitary operation into the protocol, we demonstrated how this singularity can be lifted, thereby restoring a finite and attainable bound on the estimation error. Although simultaneous estimation of multiple temperatures was not possible owing to the non-commutativity of the symmetric logarithmic derivatives (SLDs), we have introduced strategies to improve the performance compared to the individual thermal Fisher information.

Furthermore, we have determined the optimal interaction strength between the ancillary systems and the probes that maximizes the extractable joint information about the baths while maintaining a fundamental lower bound on precision. Our results also reveal that correlated ancillas can outperform uncorrelated ones provided that more than two ancillas are employed, thereby highlighting the role of multipartite correlations in quantum thermometry.

Finally, we have proposed a scalable scheme for estimating the temperatures of N independent baths by increasing the dimensionality of the ancillary systems, offering a pathway toward high-dimensional, multi-parameter quantum thermal metrology.

ACKNOWLEDGMENTS

S.G. and S.C. thank C. Mukhopadhyay and A. Das for fruitful discussions. The authors acknowledge support by MUR (Ministero dell’Università e della Ricerca) through the PNRR Project ICON-Q – Partenariato Esteso NQSTI – PE00000023 – Spoke 2 – CUP: J13C22000680006. R.L.F. also acknowledges support by MUR through the PNRR Project QUANTIP – Partenariato Esteso NQSTI – PE00000023 – Spoke 9 – CUP: E63C22002180006.

Appendix A: Importance of $U_{rot}(\theta, \hat{r})$

Let us first consider the single run scenario where the first ancilla is interacting with two probes thermalized at temperatures T_1 and T_2 . We will demonstrate here that the controlled unitary rotation in between two encodings is important to avoid the interdependencies of the two encoded parameters i.e. getting $\det\mathcal{F}_Q \neq 0$.

Considering H_{S_1} and H_{A_1} to be the system and ancilla Hamiltonian, respectively, whereas the interaction Hamiltonian giving rise to the collision is given by $H_{int}^{S_1 A_1}$. We consider

$$H_{S_1} = \frac{\omega_{S_1}}{2} \sigma_z \quad (A1)$$

$$H_{A_1} = \frac{\omega_{A_1}}{2} \sigma_z \quad (A2)$$

$$H_{int}^{S_1 A_1} = g_1 (\sigma_+ \otimes \sigma_- + \sigma_- \otimes \sigma_+) \quad (A3)$$

$$= g_1 (|01\rangle\langle 10| + |10\rangle\langle 01|) \quad (A4)$$

Thus, we have

$$\begin{aligned} U_{S_1 A_1} &= e^{-i H_{int}^{S_1 A_1} t_{S_1 A_1}^1} \\ &= |00\rangle\langle 00| + |11\rangle\langle 11| \\ &\quad + \cos g_1 t_{S_1 A_1}^1 |01\rangle\langle 01| - i \sin g_1 t_{S_1 A_1}^1 |01\rangle\langle 10| \\ &\quad - i \sin g_1 t_{S_1 A_1}^1 |10\rangle\langle 01| + \cos g_1 t_{S_1 A_1}^1 |10\rangle\langle 10| \end{aligned} \quad (A5)$$

Let us assume for simplicity $g_i = g$ and $t_{S_i A_i}^i = \tau$ for all i . Thus in the form of a matrix we get

$$U_{S_1 A_1} = \begin{bmatrix} 1 & 0 & 0 & 0 \\ 0 & \cos g\tau & -i \sin g\tau & 0 \\ 0 & i \sin g\tau & \cos g\tau & 0 \\ 0 & 0 & 0 & 1 \end{bmatrix} \quad (A6)$$

Now, notice that if we consider the ancilla state to be η and the thermalized system state to be $\rho_{th}(T_1)$, the action of the collision is given by

$$\mathcal{E}_{T_1}[\eta] = \text{Tr}_{S_1} [U_{S_1 A_1} (\rho_{th}(T_1) \otimes \eta) U_{S_1 A_1}^\dagger] \quad (A7)$$

$$\begin{aligned} &= \sum_{i=0,1} \langle i | U_{S_1 A_1} \left(\sum_{j=0,1} \lambda_j |j\rangle\langle j| \otimes \eta \right) U_{S_1 A_1}^\dagger |i\rangle_S \\ &= \sum_{i,j=0,1} \sqrt{\lambda_j} \langle i | U_{S_1 A_1} |j\rangle \eta \sqrt{\lambda_j} \langle j | U_{S_1 A_1}^\dagger |i\rangle \\ &= \sum_{i,j} K_{ij} \eta K_{ij}^\dagger \end{aligned} \quad (A8)$$

where

$$K_{ij} = \sqrt{\lambda_j} \langle i | U_{S_1 A_1} |j\rangle. \quad (A9)$$

Also note, we considered here $\rho_{th}(T_1) = \sum_i \lambda_i(T_1) |i\rangle\langle i|$ where $\lambda_i(T_1) = \mathcal{Z}(T_1)^{-1} e^{-E_i/T_1}$ where $\mathcal{Z}(T_1)$ is the partition function. Thus, we have

$$K_{00} = \sqrt{\lambda_0} (|0\rangle\langle 0| + \cos g\tau |1\rangle\langle 1|) \quad (A10)$$

$$K_{01} = -i \sin g\tau \sqrt{\lambda_1} |1\rangle\langle 0| \quad (A11)$$

$$K_{10} = i \sin g\tau \sqrt{\lambda_0} |0\rangle\langle 1| \quad (A12)$$

$$K_{11} = \sqrt{\lambda_1} (|1\rangle\langle 1| + \cos g\tau |0\rangle\langle 0|) \quad (A13)$$

We can now write down the action of Λ_T as

$$\mathcal{E}_{T_1} [|0\rangle\langle 0|] = \begin{bmatrix} \lambda_0 + \lambda_1 \cos^2 g\tau & 0 \\ 0 & \lambda_1 \sin^2 g\tau \end{bmatrix} \quad (A14)$$

$$\mathcal{E}_{T_1} [|0\rangle\langle 1|] = \begin{bmatrix} 0 & \cos g\tau \\ 0 & 0 \end{bmatrix} \quad (A15)$$

$$\mathcal{E}_{T_1} [|1\rangle\langle 0|] = \begin{bmatrix} 0 & 0 \\ \cos g\tau & 0 \end{bmatrix} \quad (A16)$$

$$\mathcal{E}_{T_1} [|1\rangle\langle 1|] = \begin{bmatrix} \lambda_0 \sin^2 g\tau & 0 \\ 0 & \lambda_1 + \lambda_0 \cos^2 g\tau \end{bmatrix} \quad (A17)$$

Thus in the vectorized form i.e. $|i\rangle\langle j| \rightarrow |ij\rangle$, we have

$$\hat{\hat{\mathcal{E}}}_{T_1} = \begin{bmatrix} \lambda_0 + \lambda_1 \cos^2 g\tau & 0 & 0 & \lambda_0 \sin^2 g\tau \\ 0 & \cos g\tau & 0 & 0 \\ 0 & 0 & \cos g\tau & 0 \\ \lambda_1 \sin^2 g\tau & 0 & 0 & \lambda_1 + \lambda_0 \cos^2 g\tau \end{bmatrix} \quad (A18)$$

Now for two consecutive collisions on the ancilla by first and the second bath, we consider $p = \lambda_0(T_1)$ for $\hat{\mathcal{E}}_{T_1}$ and $q = \lambda_0(T_2)$ for $\hat{\mathcal{E}}_{T_2}$. Thus, the action of two consecutive collisions is given by

$$\hat{\mathcal{E}}_f = \hat{\mathcal{E}}_{T_2} \cdot \hat{\mathcal{E}}_{T_1}$$

$$= \begin{bmatrix} 1 - u(T_1, T_2) & 0 & 0 & v(T_1, T_2) \\ 0 & \cos^2 g\tau & 0 & 0 \\ 0 & 0 & \cos^2 g\tau & 0 \\ u(T_1, T_2) & 0 & 0 & 1 - v(T_1, T_2) \end{bmatrix} \quad (\text{A19})$$

where

$$u(T_1, T_2) = \sin^2 g\tau [1 - p + (1 - q) \cos^2 g\tau] \quad (\text{A20})$$

$$v(T_1, T_2) = \sin^2 g\tau [p + q \cos^2 g\tau] \quad (\text{A21})$$

Now, if the initial ancilla state is $\rho_{A_1} = |1\rangle\langle 1|$, using the above, we get $\mathcal{E}_f[\rho_{A_1}] = \hat{\mathcal{E}}_f \cdot \rho_{A_1}$, so that

$$\rho_{A_1}^f = \mathcal{E}_f[\rho_{A_1}] = \begin{bmatrix} v(T_1, T_2) & 0 \\ 0 & 1 - v(T_1, T_2) \end{bmatrix}. \quad (\text{A22})$$

Thus, the SLD operators L_1 and L_2 are given by

$$L_i = \sum_{j,k=0,1} \frac{2 \langle \alpha_j | \frac{\partial \rho_{A_1}^f}{\partial T_i} | \alpha_k \rangle}{\alpha_j + \alpha_k} |\alpha_j\rangle\langle \alpha_k|, \quad (\text{A23})$$

where we have the eigenvalue decomposition $\rho_{A_1}^f = \alpha_1 |\alpha_1\rangle\langle \alpha_1| + \alpha_2 |\alpha_2\rangle\langle \alpha_2|$. Hence, for this case, we have

$$L_i = (\partial_i v) \left(\frac{1}{v} |0\rangle\langle 0| - \frac{1}{1-v} |1\rangle\langle 1| \right) \quad (\text{A24})$$

$$\text{Tr}[\eta_f L_i L_j] = \frac{(\partial_i v)(\partial_j v)}{v(1-v)} \quad (\text{A25})$$

where we used the shorthand notation ∂_i for $\frac{\partial}{\partial T_i}$.

Therefore, using this, we get

$$\mathcal{F}_Q(\eta_f) = \frac{1}{v(1-v)} \begin{bmatrix} (\partial_1 v)^2 & (\partial_1 v)(\partial_2 v) \\ (\partial_2 v)(\partial_1 v) & (\partial_2 v)^2 \end{bmatrix} \quad (\text{A26})$$

As can be easily seen here that $\det(\mathcal{F}_Q) = 0$ which would imply that the protocol automatically makes the two parameters dependent. In order to avoid this issue, we introduce a rotation $U_{rot}(\theta, \hat{r})$ between two successive collisions as shown in Fig. 1. The action of the rotation in the vectorized form is given by

$$\hat{\mathcal{U}}_{rot} = \frac{1}{2} \begin{bmatrix} 1 & i & -i & 1 \\ i & 1 & 1 & -i \\ -i & 1 & 1 & i \\ 1 & -i & i & 1 \end{bmatrix} \quad (\text{A27})$$

Thus, $\hat{\mathcal{E}}_f$ is given by

$$\hat{\mathcal{E}}_f = \hat{\mathcal{E}}_{T_2} \cdot \hat{\mathcal{U}}_{rot} \cdot \hat{\mathcal{E}}_{T_1} = \begin{bmatrix} \mu(q) & \frac{i}{2} \zeta(g) \cos g & -\frac{i}{2} \zeta(g) \cos g & \mu(q) \\ i\chi(1-p) & \frac{1}{2} \zeta(g) & \frac{1}{2} \zeta(g) & -i\chi(p) \\ -i\chi(1-p) & \frac{1}{2} \zeta(g) & \frac{1}{2} \zeta(g) & i\chi(p) \\ 1 - \mu(q) & -\frac{i}{2} \zeta(g) \cos g & \frac{i}{2} \zeta(g) \cos g & 1 - \mu(q) \end{bmatrix} \quad (\text{A28})$$

where

$$\mu(q) = \frac{1}{4}[(1+2q) + (1-2q) \cos 2g] \quad (\text{A29})$$

$$\chi(p) = \frac{1}{2}[(1-p) + p \cos 2g] \cos g \quad (\text{A30})$$

$$\zeta(g) = \cos^2 g \quad (\text{A31})$$

Thus, one can easily see that $\rho_{A_1}^f = \Lambda_f[\rho_{A_1}] = \hat{\Lambda}_f \cdot \rho_{A_1}$ is in the form

$$\rho_{A_1}^f = \begin{bmatrix} \mu(q) & -i\chi(p) \\ i\chi(p) & 1 - \mu(q) \end{bmatrix} \quad (\text{A32})$$

We will now show that $\det(\mathcal{F}_{joint}) \neq 0$ as long as $\rho_{A_1}^f$ is full

rank. Assuming $\rho_{A_1}^f$ to be full rank we have

$$\rho_{A_1}^f = \alpha_0 |\alpha_0\rangle\langle \alpha_0| + \alpha_1 |\alpha_1\rangle\langle \alpha_1| \quad (\text{A33})$$

where

$$|\alpha_k\rangle = \frac{1}{\sqrt{1+\beta_k^2}} \begin{bmatrix} 1 \\ i\beta_k \end{bmatrix} \quad (\text{A34})$$

$$\beta_k = \frac{\alpha_k - \mu}{\chi}; \quad \alpha_{0/1} = \frac{1}{2} \left[1 \pm \sqrt{1 - 4\det(\rho_{A_1}^f)} \right] \quad (\text{A35})$$

Also, note we get

$$\frac{\partial}{\partial T_1} (\rho_{A_1}^f) = \dot{\chi} \sigma_y \quad (\text{A36})$$

$$\frac{\partial}{\partial T_2} (\rho_{A_1}^f) = \dot{\mu} \sigma_z \quad (\text{A37})$$

where $\dot{\mu} = d\mu/dT_2$ and $\dot{\chi} = d\chi/dT_1$. Thus, using Theorem 1 we can see that $\det(\mathcal{F}_Q) \neq 0$. Also, we get

$$L_1 = \dot{\chi} \left\{ \frac{2\beta_0}{\alpha_0(1+\beta_0^2)} |\alpha_0\rangle\langle\alpha_0| + \frac{2\beta_1}{\alpha_1(1+\beta_1^2)} |\alpha_1\rangle\langle\alpha_1| + \frac{2(\beta_0+\beta_1)}{\sqrt{(1+\beta_0^2)(1+\beta_1^2)}} \left(|\alpha_0\rangle\langle\alpha_1| + |\alpha_1\rangle\langle\alpha_0| \right) \right\} \quad (\text{A38})$$

$$L_2 = \dot{\mu} \left\{ \frac{1-\beta_0^2}{\alpha_0(1+\beta_0^2)} |\alpha_0\rangle\langle\alpha_0| + \frac{1-\beta_1^2}{\alpha_1(1+\beta_1^2)} |\alpha_1\rangle\langle\alpha_1| + \frac{2(1-\beta_0\beta_1)}{\sqrt{(1+\beta_0^2)(1+\beta_1^2)}} \left(|\alpha_0\rangle\langle\alpha_1| + |\alpha_1\rangle\langle\alpha_0| \right) \right\} \quad (\text{A39})$$

It can be easily seen from above that $[L_1, L_2] \neq 0$ as long as $\beta_0 \neq \beta_1$, i.e., $\rho_{A_1}^f$ is full rank.

[1] M. Mehboudi, A. Sanpera, and L. A. Correa, Thermometry in the quantum regime: recent theoretical progress, *J. Phys. A: Math. Theor.* **52**, 303001 (2019).

[2] T. M. Stace, Quantum limits of thermometry, *Phys. Rev. A* **82**, 011611 (2010).

[3] M. Brunelli, S. Olivares, and M. G. A. Paris, Qubit thermometry for micromechanical resonators, *Phys. Rev. A* **84**, 032105 (2011).

[4] M. Brunelli, S. Olivares, M. Paternostro, and M. G. A. Paris, Qubit-assisted thermometry of a quantum harmonic oscillator, *Phys. Rev. A* **86**, 012125 (2012).

[5] P. P. Hofer, J. B. Brask, M. Perarnau-Llobet, and N. Brunner, Quantum thermal machine as a thermometer, *Phys. Rev. Lett.* **119**, 090603 (2017).

[6] L. A. Correa, M. Mehboudi, G. Adesso, and A. Sanpera, Individual quantum probes for optimal thermometry, *Phys. Rev. Lett.* **114**, 220405 (2015).

[7] P. A. Ivanov, Quantum thermometry with trapped ions, *Optics Communications* **436**, 101–107 (2019).

[8] J. Rubio, J. Anders, and L. A. Correa, Global quantum thermometry, *Phys. Rev. Lett.* **127**, 190402 (2021).

[9] A. De Pasquale and T. M. Stace, Quantum thermometry, in *Thermodynamics in the Quantum Regime: Fundamental Aspects and New Directions*, edited by F. Binder, L. A. Correa, C. Gogolin, J. Anders, and G. Adesso (Springer International Publishing, Cham, 2018) pp. 503–527.

[10] A. K. Pati, C. Mukhopadhyay, S. Chakraborty, and S. Ghosh, Quantum precision thermometry with weak measurements, *Phys. Rev. A* **102**, 012204 (2020).

[11] K. V. Hovhannyan, M. R. Jørgensen, G. T. Landi, A. M. Alhambra, J. B. Brask, and M. Perarnau-Llobet, Optimal quantum thermometry with coarse-grained measurements, *PRX Quantum* **2**, 020322 (2021).

[12] G. O. Alves and G. T. Landi, Bayesian estimation for collisional thermometry, *Phys. Rev. A* **105**, 012212 (2022).

[13] F. S. Luiz, A. d. O. Junior, F. F. Fanchini, and G. T. Landi, Machine classification for probe-based quantum thermometry, *Phys. Rev. A* **105**, 022413 (2022).

[14] C. W. Helstrom, Quantum detection and estimation theory, *J. Stat. Phys.* **1**, 231 (1969).

[15] M. Paris and J. Rehacek, *Quantum state estimation*, Vol. 649 (Springer Science & Business Media, 2004).

[16] V. Montenegro, C. Mukhopadhyay, R. Yousefjani, S. Sarkar, U. Mishra, M. G. Paris, and A. Bayat, Quantum metrology and sensing with many-body systems, *Phys. Rep.* **1134**, 1 (2025).

[17] F. Ciccarello, S. Lorenzo, V. Giovannetti, and G. M. Palma, Quantum collision models: Open system dynamics from repeated interactions, *Phys. Rep.* **954**, 1 (2022), quantum collision models: Open system dynamics from repeated interactions.

[18] G. Fiusa and G. T. Landi, Queued quantum collision models, *Phys. Rev. A* **111**, 032220 (2025).

[19] S. Seah, S. Nimmrichter, D. Grimmer, J. P. Santos, V. Scarani, and G. T. Landi, Collisional quantum thermometry, *Phys. Rev. Lett.* **123**, 180602 (2019).

[20] G. O. Alves, M. A. F. Santos, and G. T. Landi, Collisional thermometry for gaussian systems, *Phys. Rev. A* **110**, 052421 (2024).

[21] T. M. Mendonça, D. O. Soares-Pinto, and M. Paternostro, Information flow-enhanced precision in collisional quantum thermometry (2025), arXiv:2407.21618 [quant-ph].

[22] P. Neumann, I. Jakobi, F. Dolde, C. Burk, R. Reuter, G. Waldherr, J. Honert, T. Wolf, A. Brunner, J. H. Shim, *et al.*, High-precision nanoscale temperature sensing using single defects in diamond, *Nano letters* **13**, 2738 (2013).

[23] J.-M. Yang, H. Yang, and L. Lin, Quantum dot nano thermometers reveal heterogeneous local thermogenesis in living cells, *ACS nano* **5**, 5067 (2011).

[24] G. Kucsko, P. C. Maurer, N. Y. Yao, M. Kubo, H. J. Noh, P. K. Lo, H. Park, and M. D. Lukin, Nanometre-scale thermometry in a living cell, *Nature* **500**, 54 (2013).

[25] D. M. Toyli, C. F. de Las Casas, D. J. Christle, V. V. Dobrovitski, and D. D. Awschalom, Fluorescence thermometry enhanced by the quantum coherence of single spins in diamond, *Proceedings of the National Academy of Sciences* **110**, 8417 (2013).

[26] F. Seilmeier, M. Hauck, E. Schubert, G. Schinner, S. Beavan, and A. Högele, Optical thermometry of an electron reservoir coupled to a single quantum dot in the millikelvin range, *Phys. Rev. Appl.* **2**, 024002 (2014).

[27] F. Haupt, A. Imamoglu, and M. Krone, Single quantum dot as an optical thermometer for millikelvin temperatures, *Phys. Rev. Appl.* **2**, 024001 (2014).

[28] M. Brunelli, S. Olivares, M. Paternostro, and M. G. Paris, Qubit-assisted thermometry of a quantum harmonic oscillator, *Phys. Rev. A* **86**, 012125 (2012).

[29] C. Sabín, A. White, L. Hackermüller, and I. Fuentes, Impurities as a quantum thermometer for a bose-einstein condensate, *Sci. Rep.* **4**, 6436 (2014).

[30] A. Z. Goldberg, L. L. Sánchez-Soto, and H. Ferretti, Intrinsic sensitivity limits for multiparameter quantum metrology, *Phys. Rev. Lett.* **127**, 110501 (2021).

[31] R. Kaubruegger, A. Shankar, D. V. Vasilyev, and P. Zoller, Optimal and variational multiparameter quantum metrology and vector-field sensing, *PRX Quantum* **4**, 020333 (2023).

[32] M. Szczykulska, T. Baumgratz, and A. Datta, Multi-parameter quantum metrology, *Advances in Physics: X* **1**, 621 (2016).

[33] S. Ragy, M. Jarzyna, and R. Demkowicz-Dobrzański, Compatibility in multiparameter quantum metrology, *Phys. Rev. A* **94**, 052108 (2016).

[34] R. Demkowicz-Dobrzański, W. Górecki, and M. Guță, Multi-parameter estimation beyond quantum fisher information, *J. Phys. A: Math. Theor.* **53**, 363001 (2020).

[35] W. Górecki, S. Zhou, L. Jiang, and R. Demkowicz-Dobrzański, Optimal probes and error-correction schemes in multi-parameter quantum metrology, *Quantum* **4**, 288 (2020).

[36] J. Liu, H. Yuan, X.-M. Lu, and X. Wang, Quantum Fisher information matrix and multiparameter estimation, *J. Phys. A: Math. Theor.* **53**, 023001 (2020).

[37] F. Albarelli and R. Demkowicz-Dobrzański, Probe incompatibility in multiparameter noisy quantum metrology, *Phys. Rev. X* **12**, 011039 (2022).

[38] A. Candeloro, Z. Pazhotan, and M. G. A. Paris, Dimension matters: precision and incompatibility in multi-parameter quantum estimation models, *Quantum Science and Technology* **9**, 045045 (2024).

[39] G. Bressanini, M. G. Genoni, M. S. Kim, and M. G. A. Paris, Multi-parameter quantum estimation of single- and two-mode pure gaussian states, *J. Phys. A: Math. Theor.* **57**, 315305 (2024).

[40] C. Mukhopadhyay, A. Bayat, V. Montenegro, and M. G. A. Paris, Beating joint quantum estimation limits with stepwise multiparameter metrology (2025), arXiv:2506.06075 [quant-ph].

ph].

[41] G. Mihailescu, A. Bayat, S. Campbell, and A. K. Mitchell, Multiparameter critical quantum metrology with impurity probes, *Quantum Science and Technology* **9**, 035033 (2024).

[42] M. Gutiérrez, C. Mukhopadhyay, V. Montenegro, and A. Bayat, *Quantum error correction for multiparameter metrology* (2025), arXiv:2511.04018 [quant-ph].

[43] Y. Yang, V. Montenegro, and A. Bayat, Overcoming quantum metrology singularity through sequential measurements, *Phys. Rev. Lett.* **135**, 010401 (2025).

[44] S. Haroche and D. Kleppner, Cavity quantum electrodynamics, *Physics Today* **42**, 24 (1989).

[45] S. Haroche and J.-M. Raimond, *Exploring the quantum: atoms, cavities, and photons* (Oxford university press, 2006).

[46] M. Saffman, T. G. Walker, and K. Mølmer, Quantum information with rydberg atoms, *Rev. Mod. Phys.* **82**, 2313 (2010).

[47] A. Blais, R.-S. Huang, A. Wallraff, S. M. Girvin, and R. J. Schoelkopf, Cavity quantum electrodynamics for superconducting electrical circuits: An architecture for quantum computation, *Phys. Rev. A* **69**, 062320 (2004).

[48] A. Blais, A. L. Grimsmo, S. M. Girvin, and A. Wallraff, Circuit quantum electrodynamics, *Rev. Mod. Phys.* **93**, 025005 (2021).

[49] X. Gu, A. F. Kockum, A. Miranowicz, Y. xi Liu, and F. Nori, Microwave photonics with superconducting quantum circuits, *Physics Reports* **718-719**, 1 (2017), microwave photonics with superconducting quantum circuits.